Experimental Validation of Improved Performances of an Electromechanical Aerofin Control System With a PWM Controlled DC Motor

Milan Ristanović
Teaching and Research Assistant

Dragan Lazić
Associate Professor

University of Belgrade
Faculty of Mechanical Engineering

Ivica Inđin
Research Engineer
NIMICO DOO
Belgrade

In this paper we investigate control of an electromechanical actuator (EMA) system for aerofin control (AFC) realized with permanent magnet brush DC motor driven by a constant current driver. Using nonlinear model of the EMA-AFC system, a PID position controller was developed. During the experimental work with the EMA-AFC system we found motivation to improve performances of the system in terms of transient response and bandwidth. We proposed nonlinear PID algorithm modification. Proposed control system is experimentally validated in a test bench. Presented experimental results show that the transient response and the closed-loop frequency response with modified PID controller are considerably better compared to those obtained with conventional PID position controller.

Keywords: *Electromechanical actuator, Aerofin, DC motor, Current motor driver, PWM, PID, Simulink.*

1. INTRODUCTION

The use of electromechanical actuation is becoming increasingly popular in the aerospace industry as more importance is placed on maintainability. Electromechanical actuators (EMAs) are being used in the actuation of flight critical control surfaces and in thrust vector control. A good understanding of the dynamic properties of these actuators is critical in their successful application. Before EMA are widely accepted by the aerospace community at large for flight-critical actuation, extensive research, development, and testing must be performed, [1-3].

Direct current (DC) motors are used very often in the actuation systems of the aerodynamic surfaces. In our previous research we considered an electromechanical actuator system for aerofin control (AFC). The EMA-AFC is driven by permanent magnet brush DC motor. For this application we developed a constant current motor driver. Control signal was pulse width modulated (PWM), i.e. clipped to maximum allowed current. Physical realization of such solution is usually simpler and cheaper than the conventional voltage driver.

We introduced a SIMULINK® model of the EMA-AFC system, which takes into account non-linearties due to mechanical limitations of the fin deflection, limited motor torque and angular velocity, friction in gears and bearing, backlash in gears and lever mechanism, etc. These effects were possible to be studied by the derived nonlinear model. Using flexible SIMULINK® environment we also modeled the current motor driver, which was of great importance for understanding the behavior of the system and the control algorithm synthesis. By means of nonlinear simulation model of EMA-AFC system a PID position controller was designed.

Initially, we investigated control with conventional PID position controller, but also the other control strategies can be applied. Designed PID controller was experimentally validated in EMA-AFC testing system. We have shown that the model matches the real EMA-AFC system dynamics, thus it can be used for further investigation.

Being encouraged by experimental testing in the testing system, which provided real operating conditions, we realized that the system performances could be improved by modifying the control algorithm. We introduced nonlinear modification of the PID controller. Simulations have shown that the system performances, in terms of rise time for step or rapid inputs, tracking accuracy and bandwidth have been improved considerably.

The purpose of this paper is to give experimental validation of proposed algorithm modification.

2. AFC SYSTEM

Aerofin control (AFC) system, considered here, is the control of the missile using four grid fins. The grid fins configuration is presented in the Figure 1.

By deflecting grid fins, moments are generated about the center of mass, which in turn rotate the airframe. The resulting incidence angles generate

Received: September 2005, Accepted: February 2006.
Correspondence to: Milan Ristanović
Faculty of Mechanical Engineering,
Kraljice Marije 16, 11120 Belgrade 35, Serbia
E-mail: mristanovic@mas.bg.ac.yu

aerodynamic forces, which accelerate the vehicle in the desired direction [4].

The missile autopilot sends roll, pitch, and yaw commands (δ_x , δ_y , and δ_z) to the AFC system. Before they can be utilized, they have to be separated into individual fin commands, i.e. angles α_i, where i=0,1,2,3. Each actuator module can convert the reference fin command α_{ir}, into an actual surface deflection α_i, i=0,1,2,3. Besides, each actuator module requires tight, independent position control of the surface deflection, usually less than 10 degrees.

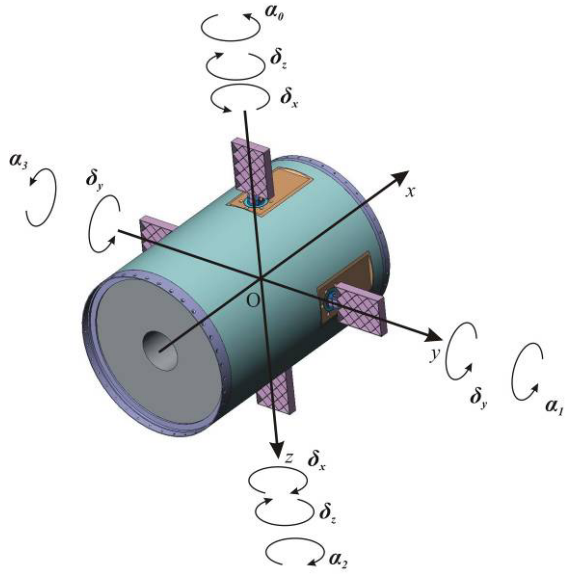

Figure 1. Actuator placement for aerofin control.

2.1 Hardware and Instrumentation

Figure 3 schematically illustrates the AFC testing system. The actuator assembly consists of the Maxon RE 30 permanent magnet brush DC motor with integrated Maxon planetary gearhead GP 32 with a 3.7 to 1 reduction, which drives the screw shaft SRCW 10 x 3 R with precision SKF roller nut SH 10 x 3 R.

The actuator assembly output shaft is connected to the roller nut via crank mechanism, driving the grid fin.

On the rear side of the motor, an incremental encoder is mounted and fixed to the rotor shaft. Incremental encoder is Maxon Encoder MR, Type M, with resolution of 256 pulses per revolution. Pulses from the encoder are forwarded to the control computer.

The control computer is actually an onboard computer (OBC) consisting of two digital signal processing (DSP) modules based on Analog Devices ADSP-21065L processor. Namely, one DSP module is used for angle measurements, while the other realizes control algorithm. All electrical connections between the DSP modules in the OBC are via motherboard. The OBC is connected with the industrial PC via serial communication, providing bi-directional transfer of set points and acquisition data. The main control loop is performed on 2 KHz sampling rate, while the serial communication operates on 500 Hz.

The OBC receives autopilot commands, converts them into individual fin angles, and based on appropriate control algorithm calculates control. Control signal is pulse width modulated, and two flags are forwarded to the motor driver.

As mentioned before, the motor driver has been designed to be simple and reliable. In order to be controlled, it needs one flag for enabling the current output, and other one for changing the current direction. The output current is adjustable, thus the driver can be used for different motors. Once, when the driver is enabled, the constant current supplies the motor, and the motor shaft rotates.

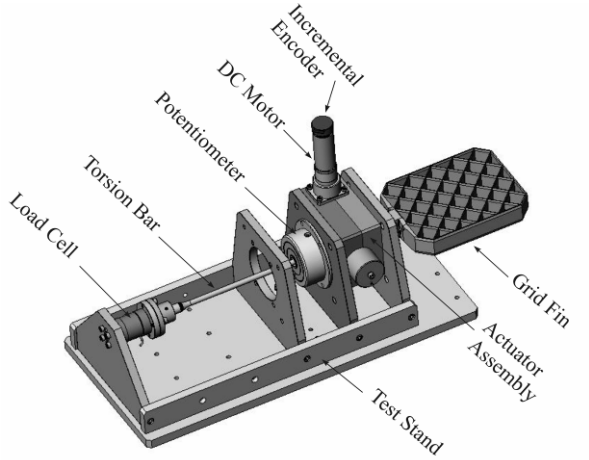

Figure 2. EMA-AFC test bench.

The motor shaft is kept around zero by providing duty cycle around 50 percent. Since the maximum current supplies the motor always, both positive and negative, the rotor shaft oscillates around zero. Having in mind the large gear ratio in the actuator assembly, the magnitude of the oscillations is attenuated, and it is negligible compared to the gear backlash.

During the design of the testing of the EMA-AFC system we have been led by an idea of simulating real load forces in the AFC system. Simulation of the real load has been especially important for testing the motor and power consumption. Hence, the EMA-AFC test bench have been designed, Figure 2.

In order to simulate inertial load, the grid fin have been mounted on the actuator assembly. The calibrated torsion bar is connected to the opposite end of the output shaft, and cantilevered with the load cell to the test bench stand. The torsion bar is designed to produce load torque induced by the aerodynamic force. It has been calibrated to give maximum torque for maximum fin deflection angle, e.g. 10 deg. Real fin angle deflection is measured by the potentiometer fixed to the output shaft. The industrial PC has acquired the load torque and deflection angle.

3. MODELING

Mathematical model of the permanent magnet DC motor can be found very often in the literature. Here, it will be referred to briefly.

The motor torque T_m is proportional to the magnetic flux, which is proportional to the armature current I_A :

$$T_m = K_M I_A , \quad (1)$$

where K_M is motor torque constant.

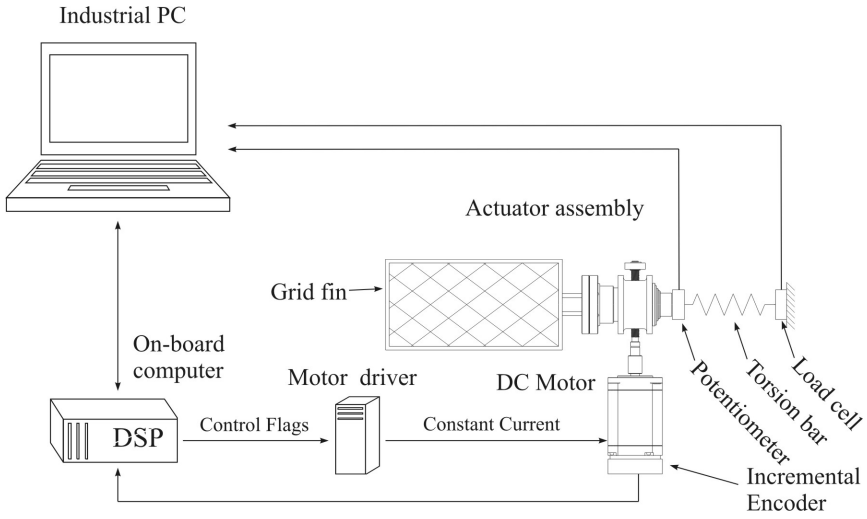

Figure 3. EMA-AFC testing system.

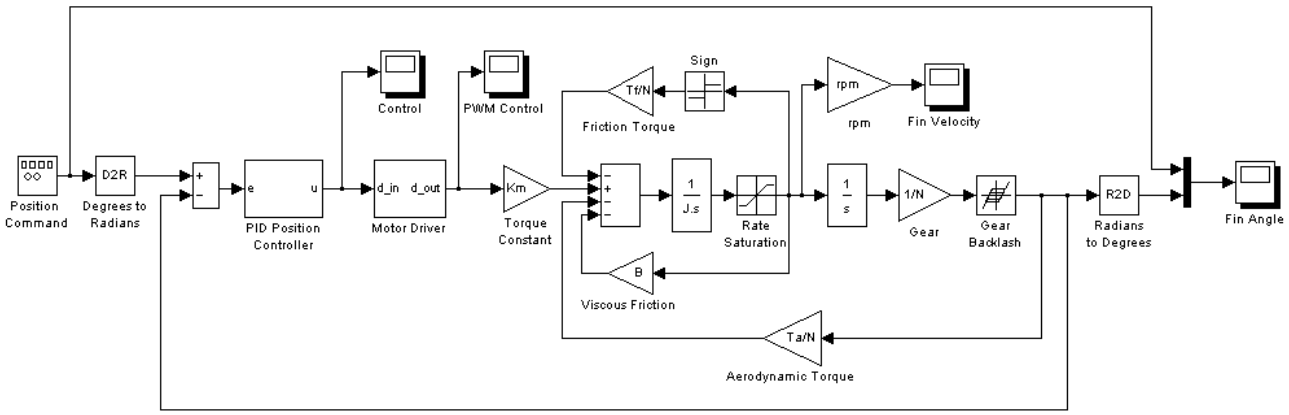

Figure 4. Simulink block diagram of EMA-AFC system.

Due to motor shaft rotation, there is induced back electromotor force E_m in the rotor coils. Back electromotor force is proportional to the rotor angular velocity ω_m:

$$E_m = K_e \omega_m , \tag{2}$$

where K_e is motor electrical constant. The torque constant and the motor electrical constant are the same for an ideal motor. For real motors, they are similar.

Voltage equation of the rotor circuitry is:

$$U_m = R_A I_A + L_A \frac{\mathrm{d}I_A}{\mathrm{d}t} + E_m , \tag{3}$$

where R_A is armature resistance, while L_A is the armature inductance.

Combining Eq. (1)-(3) yields:

$$\frac{L_A}{R_A}\frac{\mathrm{d}T_m}{\mathrm{d}t} + T_m = \frac{K_M}{R_A} U_m - K_e \omega_m . \tag{4}$$

Ratio L_A / R_A defines motor electrical time constant τ_e.

The two moments of inertia J_m and J_L are equivalent moments of inertia of the rotating motor components and the actuator assembly moment of inertia, respectively. In almost all cases, the motor inertia will be the most significant because of the large mechanical advantage of the screw drive system.

Reflecting the inertia for each of the rotating components in the actuator assembly to the motor shaft results in

$$J_L = \frac{J_{fin} + J_{lever}}{N^2 \cdot {\eta_g}^2} + J_{screw} + J_{pg} . \tag{5}$$

where J_{fin} is the fin moment of inertia, J_{lever} is the moment of inertia of the lever in screw drive mechanism, J_{screw} is the screw shaft moment of inertia, J_{pg} is the planetary gearhead moment of inertia, and η_g is the efficiency of the screw drive system.

Now, the following differential equation describes dynamics of the motor:

$$J \frac{\mathrm{d}\omega_m}{\mathrm{d}t} = T_m - T_L , \tag{6}$$

where:

$$J = J_m + J_L , \tag{7}$$

is the total moment of inertia.

Let θ_m be angle of the motor shaft rotation, then:

$$\frac{\mathrm{d}\theta_m}{\mathrm{d}t} = \omega_m \,. \tag{8}$$

Two kinds of load torques are taken into account: a friction torque and an aerodynamic torque. The friction torque can be modeled by:

$$T_{\text{fric}} = C\,\text{sign}(\dot{\theta}_m) + B\,\dot{\theta}_m \,, \tag{9}$$

where,

$$\text{sign}(\dot{\theta}_m) = \begin{cases} 1 & \text{for} \quad \dot{\theta}_m \geq 0 \\ -1 & \text{for} \quad \dot{\theta}_m < 0 \end{cases} \tag{10}$$

$$C = \frac{T_f}{N} \,. \tag{11}$$

The load torque T_{af} induced by the aerodynamic forces is proportional to the fin deflection angle α, thus:

$$T_{af} = \frac{T_a}{N}\alpha \,. \tag{12}$$

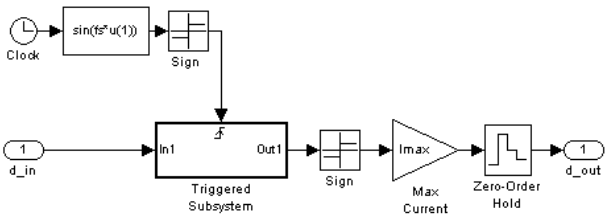

Figure 5. Simulink block diagram of the motor driver.

The factor of proportionality T_a depends on maximum aerodynamics torque and maximum fin deflection angle:

$$T_a = \frac{T_{a\max}}{\alpha_{\max}} \,. \tag{13}$$

Finally, for the screw-lever mechanism, the total gear ratio is:

$$N = \frac{2\pi}{\cos\alpha}\frac{l}{h}, \tag{14}$$

where, l is normal distance from the roller nut and the output shaft axes, and h is screw shaft pitch. Obviously, the gear ratio depends on the fin deflection angle, but for small angles it can be taken $\cos\alpha = 1$. For large angles, this approximation is usually not allowed due to considerable errors.

Equations (1) – (14) are used to develop nonlinear simulation model of the EMA-AFC system. But, the motor driver still has not been modeled. The SIMULINK® environment has been allowed effective approximation of the motor driver given in Figure 4. The continuous control signal from the OBC is sampled first on 2 KHz, and than clipped to the maximum current. The clipped current signal is held and forwarded to the motor.

Figure 4 illustrates a nonlinear model. It incorporates several nonlinear effects: gear backlash, static friction, motor shaft rate limiter and control current saturation.

The dynamics of the motor torque, defined in Eq. (4), has not been included in the nonlinear model for two reasons. First, the electrical time constant τ_e is very small, less than 1 ms. The second reason is the current motor driver, which is indifferent to induced back electromotor force. Finally, motor torque is proportional to armature current:

$$T_m = K_M I_A \,. \tag{15}$$

According to mechanical design parameters and motor specifications provided by vendor, we have following model coefficients: $J_{fin} = 1.5\cdot10^{-2}$ kg m^2, $J_{lever} = 5\cdot10^{-3}$ kg m^2, $J_{pg} = 0.15\cdot10^{-6}$ kg m^2, $J_{screw} = 5\cdot10^{-6}$ kg m^2, $J_m = 3.33\cdot10^{-6}$ kg m^2, $l = 50$ mm, $h = 3$ mm, $N = 395$, $\delta_{\max} = 10$ deg, $T_{a\max} = 19$ Nm, $T_f = 10$ Nm, $B = 0$, $K_M = 0{,}026$ Nm/A, $R_A = 0{,}611\ \Omega$, $L_A = 1.2\cdot10^{-4}$ H, $I_{\max} = 6.5$ A, $\omega_{\max} = 9500$ min^{-1}, mechanical time constant of the motor is 3 ms, and gear backlash is 0.2 deg.

4. CONTROLLER DESIGN

4.1 PID controller

Synthesis of the PID position controller, Eq. (16),

$$u(t) = K_P e(t) + K_I \int_0^\tau e(\tau)\mathrm{d}\tau + K_D \dot{e}(t) \,, \tag{16}$$

have been done using Simulink model, since it was not possible to linearize the current motor driver due to two-level current output. Hence, extensive simulation of the nonlinear model was very helpful. Parameters of PID controller were chosen to accomplish design objectives in terms of fast, non-overshooting transient response and accurate steady-state operating. Small differential gain in Eq. (16) is required because it stabilizes the system, while integral gain is responsible for steady state error. Proportional gain influences fast transient responses and it has been increased until the control reached its limitations ±2,5 V.

4.2 Modified PID controller

During the experimental testing with the EMA-AFC system we found motivation for the nonlinear algorithm modification, in order to improve response obtained with conventional PID controller.

In general, for linear systems, two broad categories of nonlinear PID control are found: those with gains modulated according to the magnitude of the state, and those with gains modulated according to the phase. Besides, nonlinear PID control has a long history and has found two broad classes of application: i) nonlinear systems where nonlinear PID control is used to accommodate the nonlinearity, often to achieve consistent response across a range of conditions; and ii) linear systems, where nonlinear PID control is used to

achieve performance not achievable by linear compensation, [5].

Here, we are interested in nonlinear PID control applied to nonlinear system with the objective of improved performance. Actually, the EMA AFC system performed well when the error signal is large, i.e. the transient response is fast, but when the error approaches zero, system becomes too slow. This is quite reasonable, because for large values of the reference input angles α_r, the load torque from aerodynamic force is maximal. In addition, there are effects of friction force and gear backlash. Since the fast response and large bandwidth is critical for the application of the EMA-AFC system, we propose the following nonlinear modification of the error signal:

$$e_c(t) = \text{sign}(e(t)) \cdot \sqrt{|e(t)|}\,. \qquad (17)$$

The error function Eq. (17) has a large gradient around zero, i.e. it behaves as scheduled parameters of the PID. Now, modified PID controller becomes

$$u(t) = K_P e_c(t) + K_I \int_0^\tau e_c(\tau)\mathrm{d}\tau + K_D \dot{e}_c(t)\,. \qquad (18)$$

4.3 Experimental validation

There have been performed experimental validations of the PID and modified PID controllers in the EMA-AFC testing system.

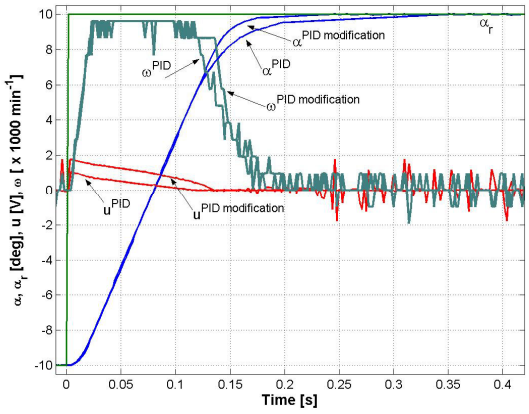

Figure 6. Square wave response on rising edge.

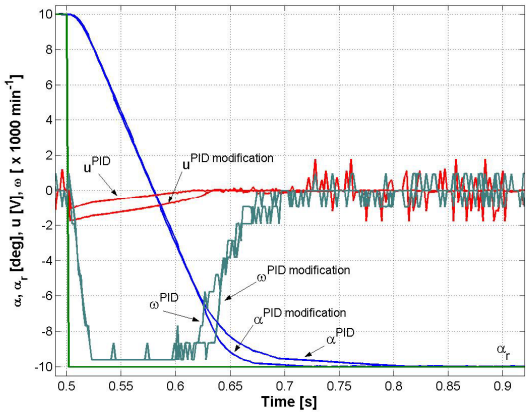

Figure 7. Square wave response on falling edge.

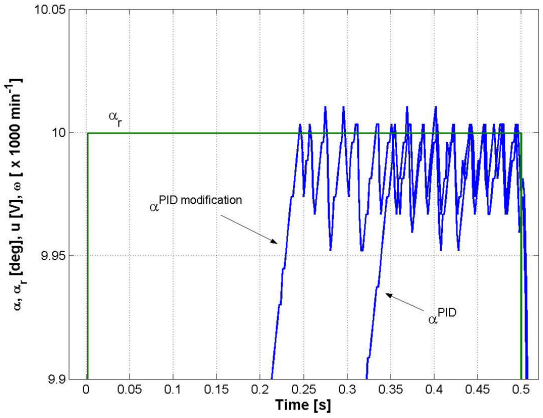

Figure 8. Steady-state accuracy on rising edge.

It has been adopted square wave reference input with the maximum allowed magnitude $|\alpha_{r\max}|$=10 deg. Parameters of the PID are selected using nonlinear simulation model to obtain maximal performances: $K_P = 1.5$, $K_I = 0.1$, $K_D = 0.1$.

Figure 6 shows response of system. It can be seen that when the error is large both controllers have the same behavior.

Modified PID controller ensures longer response with maximal shaft's angular velocity, making shorter the rising time, as well as settling time.

Similarly, in Figure 7 one can see square wave responses on falling edge. In this case, the transient response has been also increased.

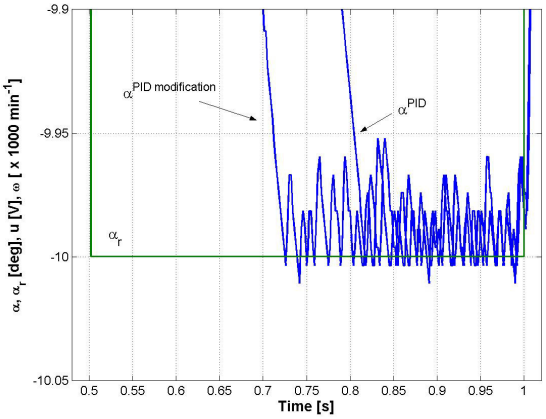

Figure 9. Steady-state accuracy on falling edge.

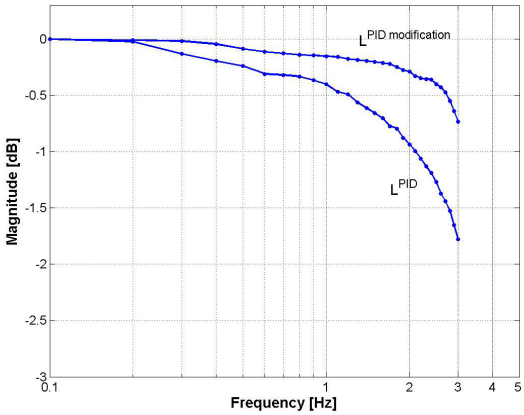

Figure 10. Experimental magnitude response of the system.

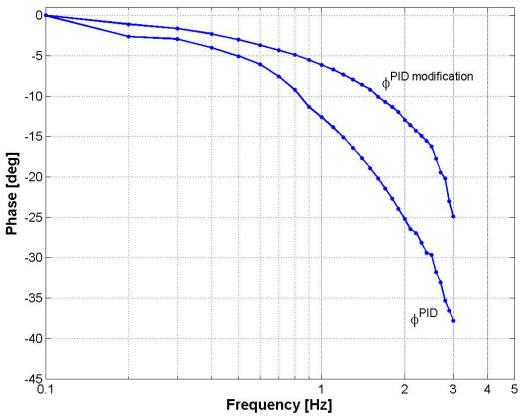

Figure 11. Experimental phase shift response of the system.

Experimental data in Figure 10 and Figure 11 define the closed-loop magnitude and phase response for the designed controller. Each data point is shown with a discrete point. The desired magnitude and frequency were changed via PC.

The steady-state accuracy can be seen in Figure 8. and Figure 9. Taking into account gear backlash, the steady-state is error and is eliminated. Also, it can be seen clearly that the settling time with modified PID is approximately 100 ms smaller than with conventional PID.

The response, together with the reference input, was sent toward the PC and recorded. Magnitude and phase have been obtained for each of the signals at the driving frequency. Presented experimental data are for the maximal magnitude of the reference 10 deg. The driving frequency has been changed from 0.1 Hz, by increments of 0.1 Hz, up to 3 Hz. The driving frequency is limited due to slow rate in response, i.e. the large total gear ratio put the motor shaft angular velocity in saturation.

According to the frequency response it is clear that modified PID controller provides broader bandwidth of the closed loop system.

5. CONCLUSION

A nonlinear model of the electromechanical actuator system for the aerofin control is used for synthesis of PID position controller. Being motivated by experimental work with the EMA-AFC testing system, we proposed nonlinear modification of the PID controller.

The validity of the proposed modification has been demonstrated in the EMA-AFC testing system simulating real operating conditions.

Present experimental results show that increased performances of the transient response are possible. In addition, the closed-loop frequency response with modified PID controller is considerably better compared to those obtained with conventional PID position controller.

ACKNOWLEDGMENT

The authors gratefully acknowledge to Mr. Milan Milisavljević, Dipl.-Ing. for mechanical design of the actuator assembly and the EMA-AFC test bench. Also, Mr. Milisavljević provided numerical data of the actuator assembly and illustrative solid model of the EMA-AFC test bench.

REFERENCES

[1] Schinstock, D. E., Douglas S. A., Haskew, T. A.: Identification of Continuous-Time, Linear, and Nonlinear Models of an Electromechanical Actuator. Journal of Propulsion and Power, Vol. 13, No. 4, p.p. 683-690. 1997.

[2] Schinstock, D. E., Douglas S. A., Haskew, T. A.: Modeling and Estimation for Electromechanical Thrust Vector Control of Rocket Engines. Journal of Propulsion and Power, Vol. 14, No. 4, p.p. 440-446. 1999.

[3] Schinstock, D. E., Haskew, T. A.: Transient Force Reduction in Electromechanical Actuators for Thrust-Vector Control. Journal of Propulsion and Power, Vol. 17, No. 1, p.p. 65-72. 2001.

[4] Zipfel, P. H.: *Modeling and Simulation of Aerospace Vehicle Dynamics,* AIAA, Reston, VA, 2000.

[5] Armstrong, B., Neevel, D., Kusik, T.: New Results in NPID Control: Tracking, Integral Control, Friction Compensation and Experimental Results. IEEE Trans. on Control Systems Technology, Vol. 9, No. 2, p.p. 399:406. 2001.

[6] Åström, K., Hägglund, T.: *PID Controllers: Theory, Design, and Tuning,* Instrument Society of America, Research Triangle Park, NC, 1995.

ЕКСПЕРИМЕНТАЛНА ПОТВРДА ПОБОЉШАЊА ПРЕЛАЗНОГ ПРОЦЕСА ЕЛЕКТРОМЕХАНИЧКОГ СИСТЕМА ЗА ПОКРЕТАЊЕ УПРАВЉАЧКОГ КРИЛА СА ШИМ УПРАВЉАНИМ МОТОРОМ ЈЕДНОСМЕРНЕ СТРУЈЕ

Милан Ристановић, Драган Лазић, Ивица Инђин

У раду се истражује управљање електро-механичког система за покретање управљачког крила изведеног са мотором једносмерне струје са четкицама и перманентним магнетом. Мотор једносмерне струје је управљан драјвером константне струје. Користећи нелинеарни модел система извршена је синтеза позиционог ПИД управљачког алгоритма. Експериментални рад са системом дао је мотивацију за побољшање прелазног процеса и пропусног опсега система. Предложена је нелинеарна модификација ПИД алгоритма управљања. Предложени управљачки систем је експериментално проверен на систему за испитивање. Приказани експериментални резултати показују да је прелазни процес и учестаносна карактеристика затвореног система знатно побољшана са модификованим ПИД алгоритмом управљања.